Rheol Acta (2002) 41: 61–76
© Springer-Verlag 2002

ORIGINAL CONTRIBUTION

Susanne E. Mall-Gleissle
Wolfgang Gleissle
Gareth H. McKinley
Hans Buggisch

The normal stress behaviour of suspensions with viscoelastic matrix fluids

Received: 20 December 2000
Accepted: 7 May 2001

S. E. Mall-Gleissle (✉)
Universitaet Karlsruhe (TH)
Institut fuer Technische Thermodynamik
und Kaeltetechnik, Engler-Bunte-Ring 21
76131 Karlsruhe
Germany
e-mail: susanne.mall-gleissle@ciw.uni-karlsruhe.de

W. Gleissle · H. Buggisch
Universitaet Karlsruhe (TH)
Institut fuer Mechanische
Verfahrenstechnik und Mechanik
76128 Karlsruhe, Germany

G. H. McKinley
Massachusetts Institute
of Technology (MIT)
Department of Mechanical Engineering
77 Massachusetts Avenue, Cambridge
MA 02139-4307, USA

Abstract We investigate the variations in the shear stress and the first and second normal stress differences of suspensions formulated with viscoelastic fluids as the suspending medium. The test materials comprise two different silicone oils for the matrix fluids and glass spheres of two different mean diameters spanning a range of volume fractions between 5 and 25%. In agreement with previous investigations, the shear stress–shear rate functions of the viscoelastic suspensions were found to be of the same form as the viscometric functions of their matrix fluids, but progressively shifted along the shear rate axis to lower shear rates with increasing solid fraction. The normal stress differences in all of the suspensions examined can be conveniently represented as functions of the shear stress in the fluid. When plotted in this form, the first normal stress difference, as measured with a cone and plate rheometer, is positive in magnitude but strongly decreases with increasing solid fraction. The contributions of the first and the second normal stress differences are separated by using normal force measurements with parallel plate fixtures in conjunction with the cone-and-plate observations. In this way it is possible for the first time to quantify successfully the variations in the second normal stress difference of viscoelastic suspensions for solid fractions of up to 25 vol.%. In contrast to measurements of the first normal stress difference, the second normal stress difference is negative with a magnitude that increases with increasing solid content. The changes in the first and second normal stress differences are also strongly correlated to each other: The relative increase in the second normal stress difference is equal to the relative decrease of the first normal stress difference at the same solid fraction. The variations of the first as well as of the second normal stress difference are represented by power law functions of the shear stress with an unique power law exponent that is independent of the solid fraction. The well known edge effects that arise in cone-and-plate as well as parallel-plate rheometry and limit the accessible measuring range in highly viscoelastic materials to low shear rates could be partially suppressed by utilizing a custom-designed guard-ring arrangement. A procedure to correct the guard-ring influence on torque and normal force measurements is also presented.

Key words Viscoelastic suspension · Highly filled material · First normal stress difference · Second normal stress difference · Normal stress product · Edge fracture

Introduction

Due to their prevalence in commercial processing operations, there is a continuing interest in understanding the viscometric properties of highly filled viscoelastic fluids. The normal stress differences in suspensions based on viscoelastic matrix fluids are often of similar magnitude as the shear stress, even at low shear rates. The resulting stress distributions arising in a complex flow such as capillary due or extruder affect a number of important processing criteria which are commonly grouped under the broad heading of 'processability'. Relevant parameters may include the recoverable shear, the magnitude of the extrudate swell, and the critical conditions for onset of flow instabilities. Further considerations are provided in the recent review of Hornsby (1999).

The theoretical description of the normal stress differences in concentrated suspensions formulated with Newtonian suspending fluids is now fairly well understood. The magnitude and sign of the normal stress differences depends on the magnitude of the dimensionless shear rate, or Peclet number, measuring the relative importance of the imposed viscous shear stress and Brownian motion. Theoretical scaling arguments and Stokesian dynamics calculations show that in colloidal dispersions the normal stress differences vary linearly with the magnitude of the deformation rate at very small dimensionless shear rates. At higher Peclet numbers the normal stress behaviour becomes more complex with shear thinning and the possibility of changes in sign at high deformation rates (for further details see Brady and Vicic 1995; Phan-Thien et al. 1999; Foss and Brady 2000). Careful viscometric measurements in a number of different torsional flow configurations using suspensions with viscous, but Newtonian, matrix fluids appear to support the model predictions at high Peclet numbers (Zarraga et al. 2000).

Much less is known theoretically or experimentally about the normal stress differences in highly-filled suspensions formulated with viscoelastic matrix fluids. The first normal stress difference behaviour of suspensions has been quantified for some materials such as filled rubbers (Tanaka and White 1980); however instabilities such as edge fracture typically limit the range of deformation rates that can be examined. There are a few publications indicating that the second normal stress differences in viscoelastic suspensions may be higher in magnitude than in the pure liquid and may even overcome the magnitude of the first normal stress difference (Tanaka and White 1980; Ohl and Gleissle 1992). In the most comprehensive investigation to date, Aral and Kalyon (1997) examined a number of rheological properties for viscoelastic suspensions formulated using hollow spherical glass beads in a highly viscous silicone oil over a broad range of volume fractions ($0.1 \leq c_v \leq 0.6$). For volume fractions above 30% the first normal stress difference measured in steady torsional shear flow was found to be negative with a magnitude that increased with deformation rate and volume fraction. At very large volume fractions ($c_v > 0.4$) additional complexities such as the failure of time-temperature superposition and the presence of a measurable yield stress were documented. Negative normal stress differences ($N_1 - N_2$) > 10 kPa have also been measured in glass bead-silicone oil suspensions from Gleissle (1996).

Microstructural modeling of such viscoelastic phenomena are just beginning; however, Brownian dynamics calculations using a linear viscoelastic (Maxwell) matrix fluid appear to agree with some of the experimental observations of Aral and Kalyon for small imposed deformations (Schaink et al. 2000). However, theoretical consideration of the effects of normal stress differences generated in the matrix fluid at large imposed shear strains have yet to be considered. It is to be hoped that experimental measurements of general rheological trends or scaling results for filled viscoelastic fluids might be used to guide future theoretical considerations.

One common experimental observation is that the first normal stress difference in a filled viscoelastic fluid is a power-law function of the imposed shear stress such that $N_1 \approx \tau^n$ with a power-law exponent (n) that appears to depend on the specific matrix fluid used in preparing the suspension. Ohl and Gleissle (1992, 1993) obtained values of $n \approx 1.6$ for glass spheres in viscoelastic silicone oils using torsional flows in the cone-and-plate and parallel-plate geometries. Markovic et al. (2000) used measurements of the recoverable shear and the wall shear stress in a capillary extrusion geometry to infer a value of $n \approx 1.3$ for a number of ethylene-propylene-diene (EPDM) rubbers and a wide range of different curing formulations. Liang and Li (1999) used capillary rheometry measurements in glass-bead filled LDPE composites and found $n \approx 1$ for volume fractions between 10 and 40 vol.%. Corresponding measurements of the second normal stress difference are much scarcer due to the need for special rheometric techniques (see, for example, Petersen 1974; Lee et al. 1992). One of the principal goals of this paper is to quantify the first and the second normal stress differences of filled viscoelastic fluids and to show that there are strong correlations between the variations in N_1 and N_2 with both deformation rate and volume fraction of filler. A new material constant is introduced which combines information about both N_1 and N_2, and which is independent of the solid filler fraction (Gleissle et al. 1998, 2000).

Materials and methods

To investigate the shear and the normal stress behaviour of filled materials with viscoelastic matrix fluids, two groups of model

suspensions were formulated. The first series consists of a silicone oil matrix with a zero-shear-viscosity $\eta_0 = 10^3$ Pa s (AK10^6 Wacker Chemie) filled with sieved glass beads of $\bar{x} = 4$ μm average diameter. The second group was formulated with a lower viscosity silicone oil with $\eta_0 = 400$ Pa s (DOW 3 · 10^5 Dow-Corning) and monodisperse glass spheres of $\bar{x} = 0.5$ μm diameter. The volume-fraction c_v of the solid has been varied between $0 \leq c_v \leq 25\,\%$.

A torsional rheometer (Rheometric Scientific RMS 800) was used to measure the three viscometric functions; i.e., the shear stress $\tau(\dot{\gamma})$, and the first and second normal stress differences $N_1(\dot{\gamma})$ and $N_2(\dot{\gamma})$. This rate-controlled instrument is equipped with a rebalance torque and force transducer. A variety of cone-and-plate as well as plate-and-plate fixtures have been used. The dimensions of the different geometries are given in Table 1.

The shear stress functions (from CP and PP fixtures)

Agreement between the shear stress functions measured using cone-and-plate (CP) fixtures and parallel-plate (PP) fixtures (denoted henceforth τ_{CP} and τ_{PP}) was first tested. Here τ_{PP} is the true steady state shear stress at the rim ($r = R$) in a parallel plate device. If M_{CP} and M_{PP} are the torques measured in the CP- and PP-devices respectively then

$$\tau_{CP} = \frac{3}{2\pi R^3} \cdot M_{CP} \tag{1}$$

$$\tau_{PP} = \frac{M_{PP}}{2\pi R^3}\left(3 + \frac{\mathrm{d}\ln M_{PP}}{\mathrm{d}\ln \dot{\gamma}}\right) . \tag{2}$$

For further details see for example Bird et al. (1987) or Powell (1998).

The resulting shear stresses of the virgin silicone oil AK 10^6 and a series of suspensions formulated using this fluid as the suspending matrix fluid are plotted as a function of the shear rate in Fig. 1. The data demonstrate that the measurements with CP- and PP geometries give equivalent results as expected. Deviations between CP- and PP results are within the magnitude of the plotting symbols. This agreement is of fundamental importance for the method used to separate N_1 and N_2 (with CP and PP measurements) as described later.

It is commonly appreciated that viscoelastic liquids with large normal stresses tend to exhibit flow instabilities in steady torsional shear flow which limit the maximum shear rate achievable (Hutton 1969; Gleissle 1974; Tanner and Keentok 1983). It is now generally accepted that these instabilities result from the action of the second normal stress difference on defects naturally arising at the free surface at the outer rim of a cone-and-plate or parallel-and-plate fixture (Lee et al. 1992; Keentok and Xue 1999). Similar edge fracture instabilities are also observed in filled suspensions formulated using Newtonian suspending fluids and also appear to correlate well with the magnitude of the (negative) second normal stress difference (Zarraga et al. 2000). To avoid these instabilities and to extend the measuring range towards higher shear rates or shear stresses, a special guard-ring assembly was constructed as shown in Fig. 2. This fixture was based on the designs of Gleissle (1976, 1978) and removes the free surface from the edge of the fixture. The modified geometry and increased gap between the stationary and rotating surfaces shifts the critical condition for onset of instability to higher deformation rates. Using this guard-ring the measuring range could be extended by a factor of approximately two or three.

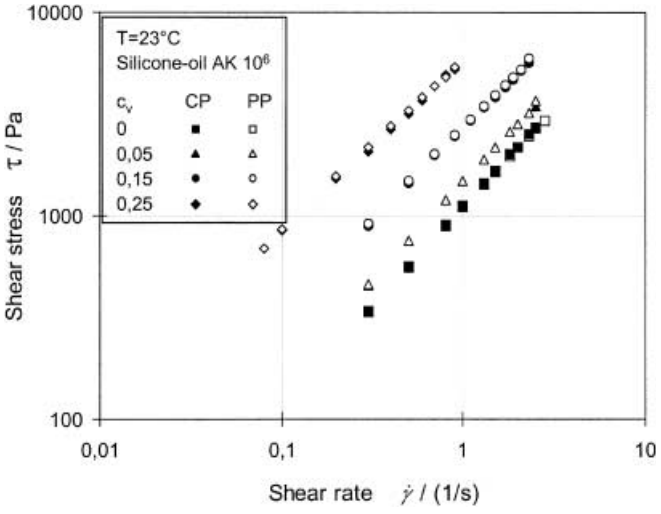

Fig. 1 Flow curves for the AK 10^6 matrix fluid and suspensions with $c_v = 0.05$, 0.15, 0.25 measured in cone-and-plate and parallel-plate geometries

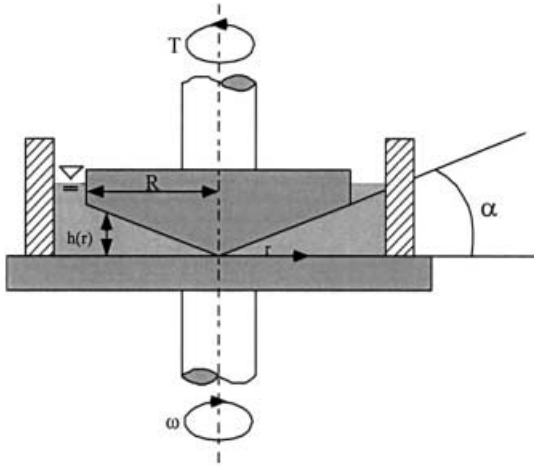

Fig. 2 Schematic drawing of the guard-ring assembly employed to increase the range of shear rates attainable before onset of edge fracture

Table 1 Dimensions of the cone-and-plate (CP) and parallel-plate (PP) rheometer fixtures used in this study

DOW 3 · 10^5 c_v	CP R/mm	α/°	PP R/mm	H/mm	AK 10^6 c_v	CP R/mm	α/°	PP R/mm	H/mm
0	30	2.3	30	1.1	0	12.5	5.7	12.5	1.05
0.125	12.5	5.7	30	1.35	0.05	12.5	5.7	12.5	1.0
0.18	12.5	5.7	30	1.05	0.15	12.5	5.7	12.5	1.0
0.25	12.5	5.7	30	1.05	0.25	12.5	5.7	12.5	0.9

Quantitative measurement of the shear stress using the guard-ring assembly requires a rim-correction because of the additional torque resulting from the fluid in the region between the shear gap and the guard-ring. The correction factor can be obtained from data obtained in a matching or overlap region (i.e., from measurements of the torque at the same shear rate in geometries with and without the guard-ring). The validity of this correction factor can be independently checked with the normal stress measurements as we discuss below.

The shear stress functions $\tau(\dot{\gamma}, c_v)$ of AK 10^6 and the corresponding series of filled suspensions are shown in Fig. 3.

The data shown in Fig. 3 appear to be self-similar and simply shifted parallel to each other along the shear-rate axis. By utilizing the concept of the shear-stress-equivalent internal shear rate (Gleissle and Baloch 1984) the viscometric functions of the suspensions can be represented by one single master curve by shifting the curves laterally along the rate axis by a factor B_τ. This shift is defined in Eq. (3) below and is best interpreted as a shear rate amplification factor:

$$B_\tau(c_v) = \left(\frac{\dot{\gamma}_m}{\dot{\gamma}_{susp}(c_v)} \right)\Bigg|_\tau \tag{3}$$

The amplification is given by the ratio of the shear rate $\dot{\gamma}_m$ in the viscous Newtonian matrix fluid to the shear rate $\dot{\gamma}_{susp}$ developed in the suspension at the same externally-imposed shear stress. The factor B_τ is a dimensionless shift factor scaling the average increase of the true internal shear rate $\dot{\gamma}_{\text{int}} \equiv B_\tau \dot{\gamma}_{susp}$ because of the presence of rigid particles. The master curves resulting from shifting of the experimentally measured shear stress functions for both series of suspensions onto the representative viscometric functions of the suspending matrix fluids are presented in Fig. 4.

Normal stress differences

One consequence of the homogenous shear rate generated in a cone-and-plate-rheometer is the direct proportionality of the first normal stress difference to the total axial force or thrust F_{CP}, exerted on the fixtures:

$$N_1 = \frac{2}{\pi R^2} \cdot F_{CP} \tag{4}$$

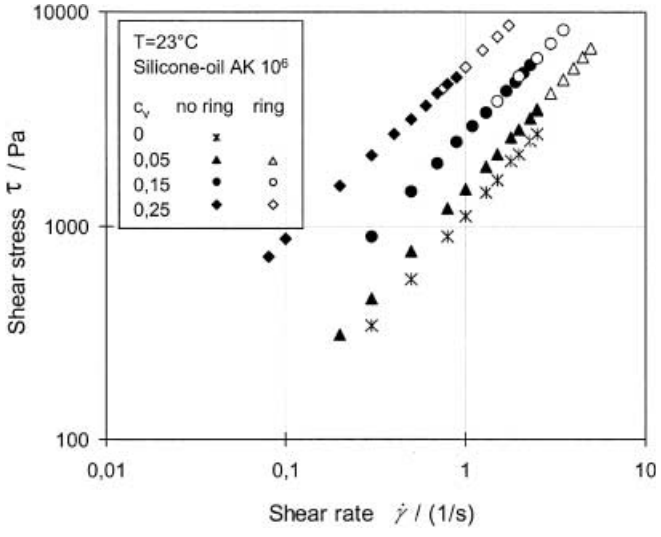

Fig. 3 Shear stress functions of AK 10^6 matrix fluid and suspensions with $c_v = 0.05$, 0.15, 0.25 measured with and without the guard-ring

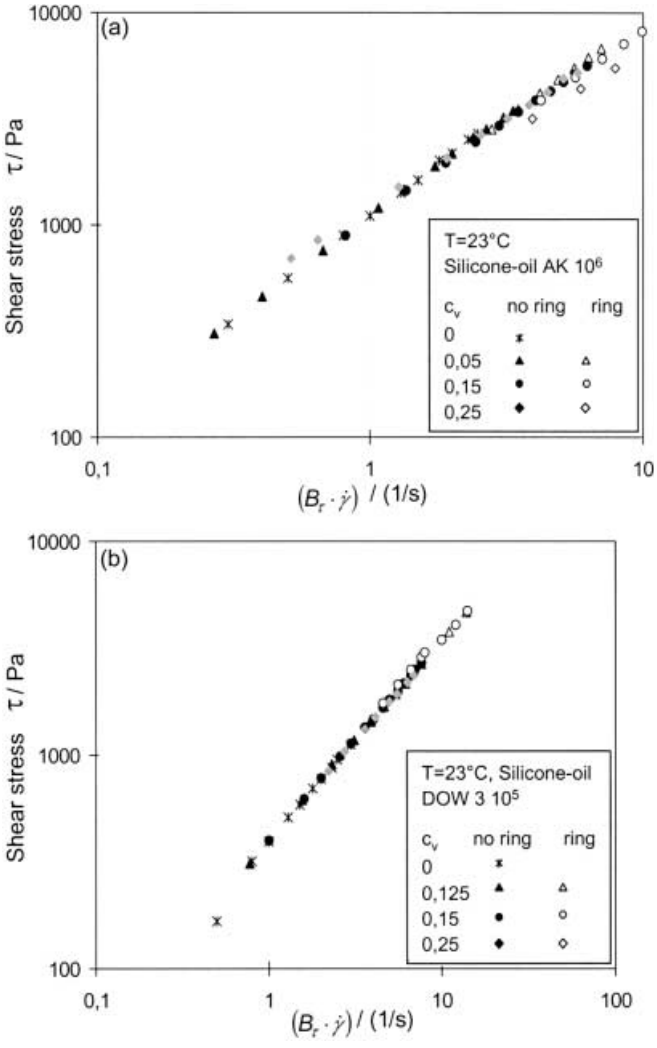

Fig. 4a, b Master curves of the shear stress as a function of shear rate for filled suspensions over a range of volume fractions ($0 \le c_v \le 0.25$) formulated with two viscoelastic matrix fluids: **a** AK 10^6 silicone oil; **b** DOW $3 \cdot 10^5$ silicone oil

The more complex analysis required for the nonhomogeneous shear flow in the parallel-plate device leads to a relationship between the total axial force F_{PP} and the difference between the first and the second normal stress differences $N_1 - N_2$ that can be expressed in the form (Kotaka et al. 1959; Bird et al. 1987)

$$(N_1(\dot{\gamma}_R) - N_2(\dot{\gamma}_R)) = \left(\tfrac{F_{PP}}{\pi R^2}\right) \cdot \left\{ 2 + \tfrac{\mathrm{d} \ln F_{PP}}{\mathrm{d} \ln \dot{\gamma}_R} \right\} \tag{5}$$

where R is the radius of the plates, H is the plate separation and $\dot{\gamma}_R \equiv \Omega R/H$ is the maximum or rim shear rate at the edge of the fixture. For a second-order fluid or convected Maxwell model with $N_1 - N_2 \sim \dot{\gamma}^2$, Eq. (5) can be reduced to the simple form:

$$(N_1(\dot{\gamma}_R) - N_2(\dot{\gamma}_R)) = \frac{4}{\pi R^2} \cdot F_{PP} \tag{6}$$

If the first normal stress difference $N_1(\dot{\gamma})$ is known from cone-and-plate measurements then the second normal stress difference $N_2(\dot{\gamma})$ can, in principle, be separated from parallel-plate measurements of $(N_1 - N_2)_{\dot{\gamma}}$. Combining Eqs. (4) and (6) one obtains:

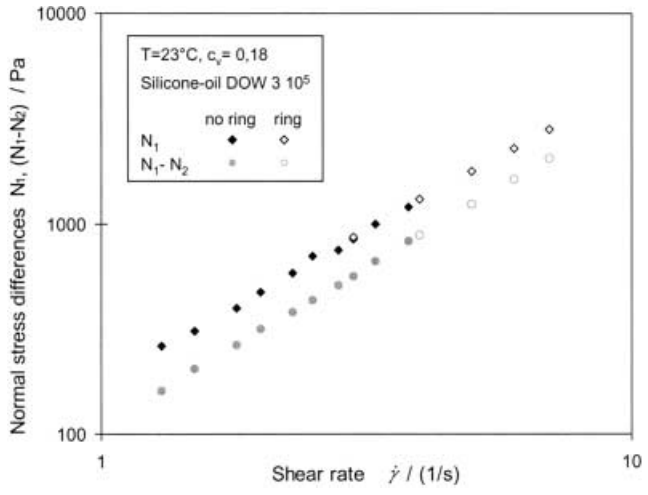

Fig. 5 Normal stress differences $N_1^{(CP)}$ and $(N_1 - N_2)^{(PP)}$ measured as a function of imposed shear rate with, and without, the guard-ring assembly

$$N_2(\dot{\gamma}_R) = \frac{F_{CP}}{\pi R_{CP}^2} - \frac{F_{PP}}{\pi R_{PP}^2}\left\{2 + \frac{\mathrm{d}\ln F_{PP}}{\mathrm{d}\ln \dot{\gamma}_R}\right\} \tag{7}$$

This procedure can be difficult to carry out reliably in practice since the second normal stress difference for polymer solutions is typically small and the two terms are comparable in magnitude (Meissner et al. 1989). However, if the second normal stress is comparable in magnitude to the first normal stress difference (regardless of sign), then such an analysis can be accurately performed (Zarraga et al. 2000). This is the method we have applied to separate $N_1(\dot{\gamma})$ and $N_2(\dot{\gamma})$ from the axial force measurements in cone-and-plate- and parallel-plate measurements.

As we have discussed above, the experimentally accessible window can be extended to higher shear rates using a guard-ring to avoid edge fracture instabilities. However, there is consequently a need to correct the values of shear stresses calculated from torque measurements with the guard-ring. As a result of the geometry of this assembly there should be almost no influence of the guard-ring on the axial force. Normal force measurements confirm these assumptions for both the CP- and the PP-fixtures as demonstrated in Fig. 5, where the functions $N_1(\dot{\gamma})$ and $N_1 - N_2$ computed using Eqs. (4) and (5) are plotted as a function of the imposed shear rate $\dot{\gamma}$.

However, if N_1 and $N_1 - N_2$ are compared at fixed values of the shear stress, differences are found between measurements with and without guard-ring as shown in Fig. 6.

As a result of the additional torque generated by the guard-ring system the shear stress computed from the torque requires a rim-correction procedure. This correction can be readily performed by shifting the values of $N_1(\tau)^{[ring]}$ and $(N_1(\tau) - N_2(\tau))^{[ring]}$ horizontally along the abscissa towards lower stresses. The appropriate value of the rim-correction factor is obtained in the overlapping region. The resulting correction factors coincide with the correction factors obtained from Fig. 3 for the shear stress. This rim-correction procedure leads to straight lines for log N_1 and log $N_1 - N_2$ as functions of log τ as has previously been observed by Tanaka and White (1980) and Ohl and Gleissle (1993).

The transient evolution in the material functions can also be followed using step changes in the deformation rate. Representative plots showing the temporal evolution in the normal stress functions are shown in Fig. 7 following inception of steady shear flow. The

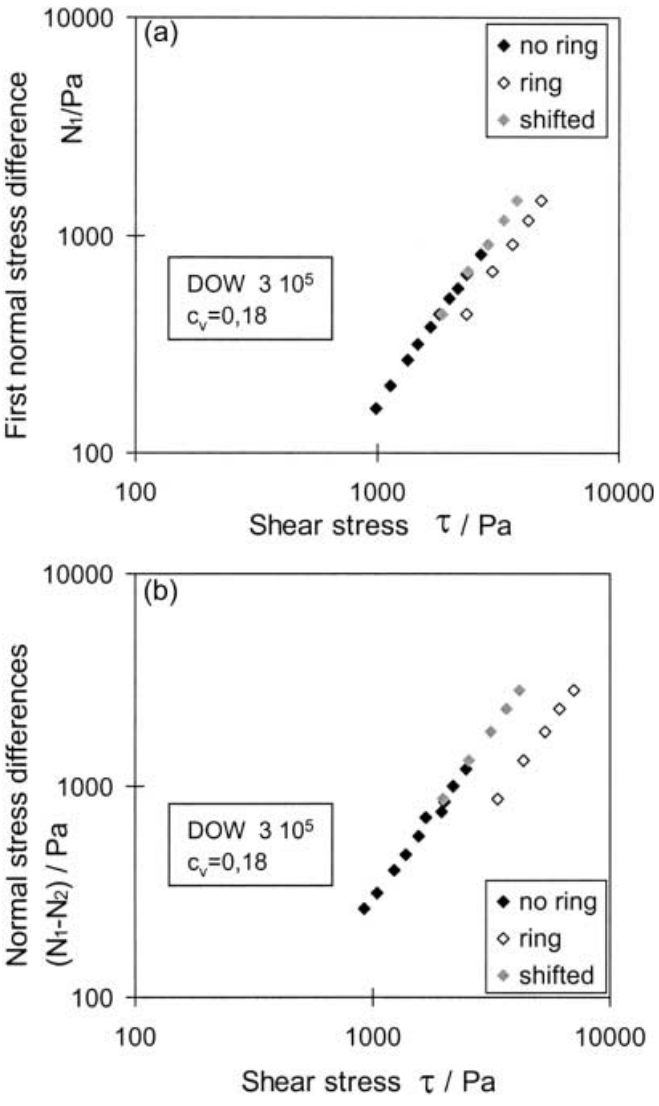

Fig. 6a, b Normal stress differences $N_1(\tau)$ and $(N_1(\tau) - N_2(\tau))$ measured with, and without, guard-ring showing the shift in the material functions resulting from the extra torque associated with the fluid between the guard-ring and the rheometer fixture

results are typical of those expected for concentrated polymer solutions with stress overshoots occurring at higher shear rates. In contrast to the experiments of Aral and Kalyon (1997) we do not observe changes in sign of the normal stress differences with time when using the guard ring assembly. The contributions of the first and the second normal stress differences to the total normal force in the PP geometry can be separated using the average values of the forces obtained in the steady-state region of these curves. Although this procedure can also be applied to the transient force signals, the resulting material functions are best interpreted as 'apparent' values of $N_1^+(\dot{\gamma}_0, t)$ and $N_2^+(\dot{\gamma}_0, t)$ since Eq. (7) was obtained assuming a steady shearing deformation. Different values of the elapsed time prior to reaching steady state are used for the calculation of the average force values at different shear rates because of the onset of edge fracture instabilities at high shear rates after a certain time.

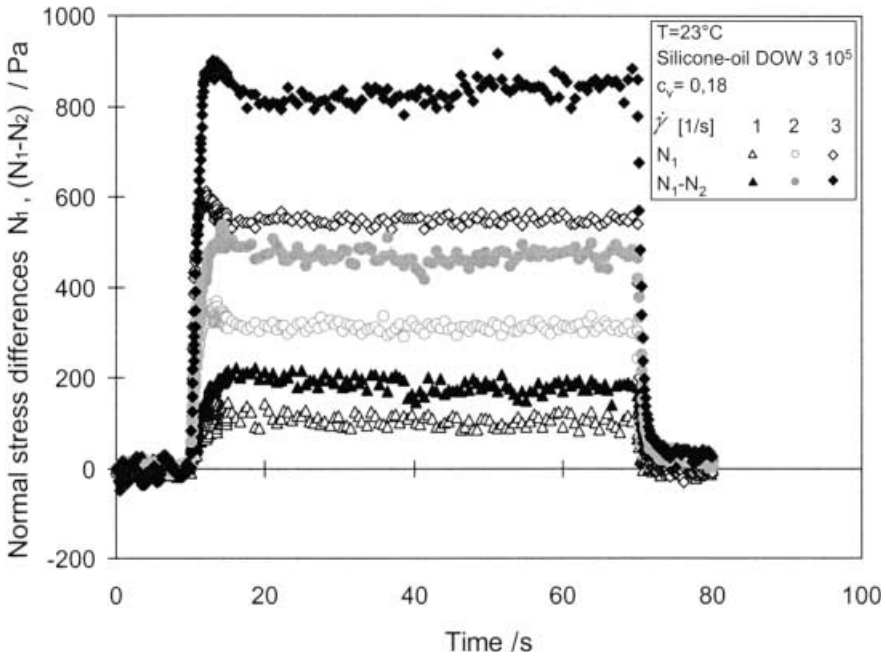

Fig. 7 Transient evolution of the first normal stress difference $N_1^+(t,\dot{\gamma})$ in the cone-and-plate geometry and the apparent normal stress difference $(N_1 - N_2)^+$ computed from the thrust measured in the parallel-plate geometry (cf. Eq. 6) at different applied shear rates

Results and discussion

The normal stress differences of the pure matrix fluids as functions of the shear stress

The normal stress-shear stress functions $N_1(\tau)$ of the silicone oil DOW $3 \cdot 10^5$ and $N_1(\tau)$ and $|N_2(\tau)|$ of AK 10^6 result in straight lines in a double-logarithmic plot as indicated in Fig. 8. The second normal stress difference for the more viscoelastic AK 10^6 oil was found to be negative at all deformation rates with a magnitude of approximately $0.1 \cdot N_1$ (when compared at the same value of the applied stress). It was not possible to measure reliably the function $N_2(\tau)$ for the less viscous silicone oil due to its small magnitude.

The data in Fig. 8 suggests that the functions $N_1(\tau)$ and $|N_2(\tau)|$ can be represented by power law functions of the form:

$$N_1 = a_{N_1,m} \cdot \tau^{n_1} \tag{8}$$

$$|N_2| = a_{N_2,m} \cdot \tau^{n_2} \tag{9}$$

Equation (8) agrees with results published by Tanaka and White (1980), Ohl (1991), and Ohl and Gleissle (1993). The data in Fig. 8 suggest that the power law exponent n_1 is independent of the type of silicone oil and that the power law exponent n_2 for the second normal stress difference appears to be similar in magnitude to n_1. Numerical values of these power law exponents n_1 and n_2 for the pure matrix fluids are given together with the results of the filled suspensions below.

First normal stress difference as a function of the solid fraction

The first normal stress-shear stress functions $N_1(\tau, c_v)$ shown in Figs. 9 and 10 for the silicone oils DOW $3 \cdot 10^5$ and AK 10^6 and for the corresponding glass-bead suspensions exhibit the behaviour expected from previous investigations. The magnitude of the first normal stress differences N_1 (c_v) decreases with increasing solid fraction c_v when compared at constant values of the imposed shear stress τ. In other words, the normal stress difference may increase with filler volume fraction but not as fast as the shear stress does.

The data reveals that a set of parallel straight lines are found in plots of log N_1 – log τ regardless of the solid volume-fraction c_v. Hence the evolution in the normal stress function N_1 (τ) can be written compactly in the form

$$N_1(c_v, \tau) = a_{N_1}(c_v) \cdot \tau^{n_1} \qquad n_1 \neq f(c_v) \tag{10}$$

and the data are represented by power laws with a power law exponent n_1 that is independent of the solid volume fraction c_v. These observations are in agreement with previously published results of Tanaka and White (1980), Ohl (1991), and Ohl and Gleissle (1993).

The expressions in Eqs. (8) and (10) at a fixed value of the imposed shear stress can thus be expressed in terms of a *first normal stress shift factor* defined by

$$\left.\frac{N_1(c_v = 0)}{N_1(c_v)}\right|_\tau \equiv B_{N_1}(c_v)\,|_\tau = \frac{a_{N_1,m}}{a_{N_1}(c_v)}. \tag{11}$$

The ratios B_{N_1} (c_v) defined by Eq. (11) give the factor by which the normal stress function $N_1(\tau, c_v = 0)$ of the

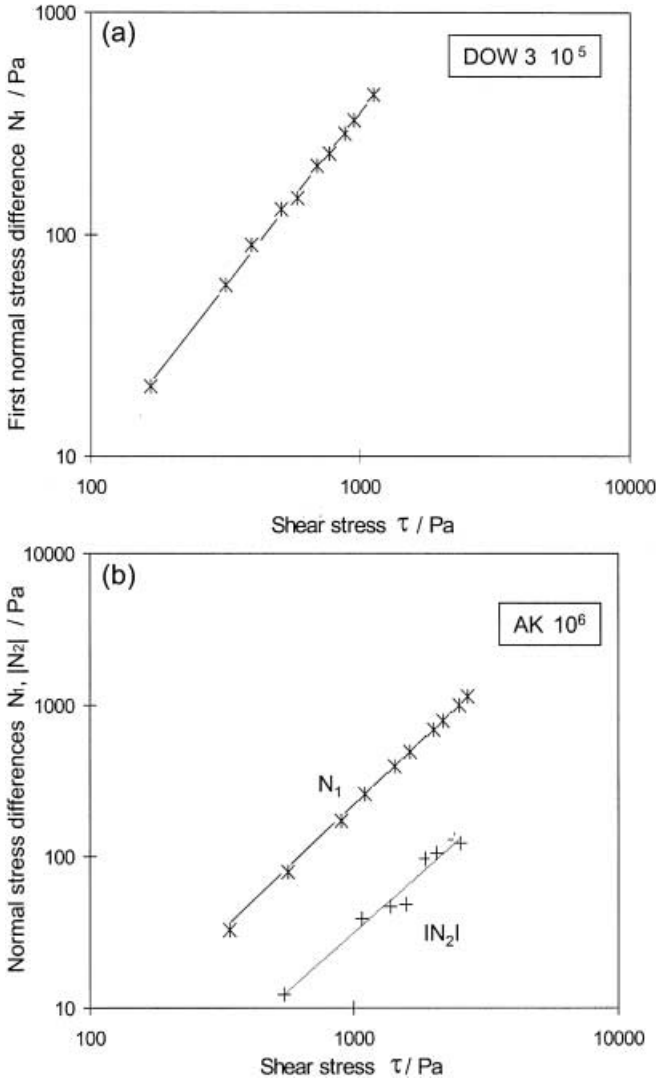

Fig. 8a, b First normal stress differences $N_1(\tau)$ of the polymeric solvents used as suspending fluids: **a** DOW $3 \cdot 10^5$; **b** AK 10^6. The second normal stress difference $|N_2(\tau)|$ for the AK 10^6 matrix fluid is also shown in b but could not be reliably measured for the less viscous fluid

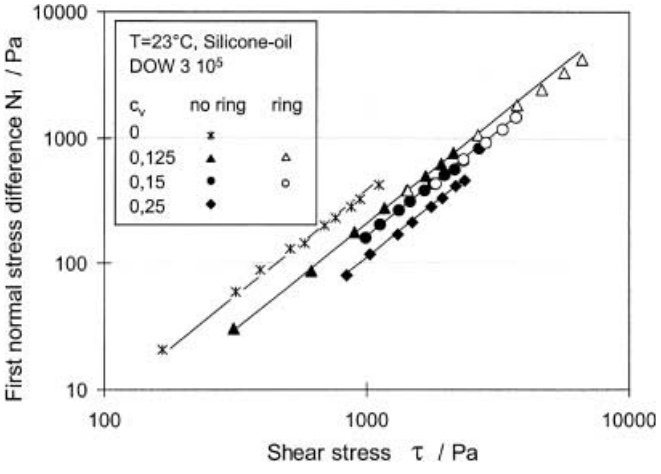

Fig. 9 Variation in the first normal stress difference $N_1(\tau)$ of glass-bead filled suspensions formulated using the DOW $3 \cdot 10^5$ matrix fluid

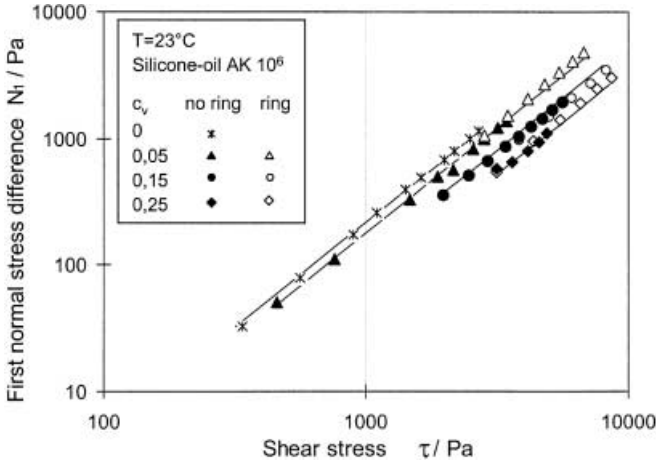

Fig. 10 The first normal stress differences $N_1(\tau)$ of glass-bead filled suspensions formulated using the AK 10^6 matrix fluid

pure matrix fluid is shifted downwards on a double logarithmic plot with increasing c_v. The numerical value of the shift factor is independent of the imposed shear stress and consequently the first normal stress functions of all the viscoelastic suspensions $N_1(\tau, c_v)$ can be written in the compact reduced form

$$N_1(c_v, \tau) = \frac{a_{N_1,m}}{B_{N_1}(c_v)} \cdot \tau^{n_1}. \qquad (12)$$

The influence of the suspended rigid particles on the viscometric function $N_1(\tau)$ is quantified by a single scalar number $B_{N_1}(c_v)$ that is independent of the shear stress (and the shear rate) and only a function of the volume fraction of filler.

Second normal stress difference as a function of the solid fraction

Combining the thrust measurements in the cone-and-plate and parallel plate geometries, we are also able to systematically evaluate the second normal stress difference N_2 for the filled suspensions. The second normal stress is found to be negative (as for the pure viscoelastic fluids) in all our measurements and hence in double logarithmic plots we plot the magnitude of N_2.

Measurements for the two series of filled suspensions are shown in Figs. 11 and 12. Although the shapes of the curves are similar to those of the first normal stress difference, the magnitude of N_2 is found to grow with increasing solid volume fraction. The viscometric functions for each volume fraction form parallel straight lines in double logarithmic plots of log $|N_2|$ vs log τ. The

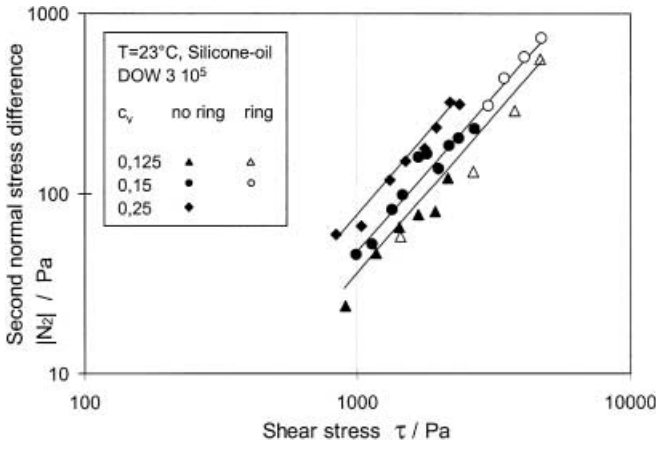

Fig. 11 The second normal stress difference $N_2(\tau)$ of glass-bead filled suspensions formulated using the DOW $3 \cdot 10^5$ matrix fluid

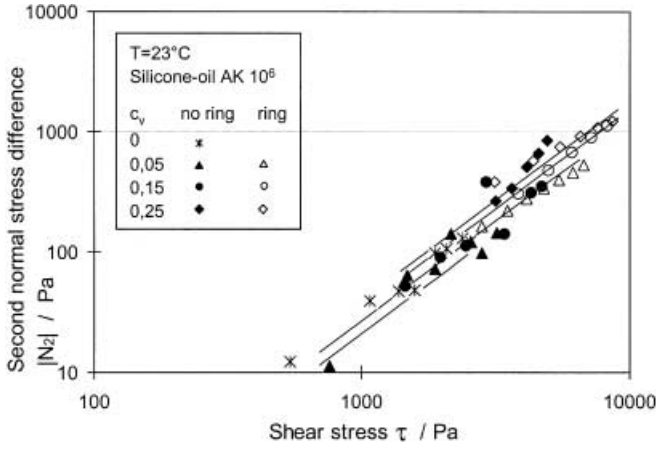

Fig. 12 The second normal stress difference $N_2(\tau)$ of glass-bead filled suspensions formulated using the AK 10^6 matrix fluid

variation in the second normal stress difference can therefore also be described by a power law function with a single exponent n_2 that is applicable to all concentrations examined:

$$|N_2| = a_{N_2}(c_v) \cdot \tau^{n_2} \qquad n_2 \neq f(c_v) \tag{13}$$

The magnitude of the shift along the ordinate axis can again be written in terms of a shift factor $B_{N_2}(c_v)$ that is independent of the shear stress and varies with increasing solid fraction as

$$\left.\frac{N_2(c_v = 0)}{N_2(c_v)}\right|_{\tau} \equiv B_{N_2}(c_v) \quad . \tag{14}$$

Consequently the viscometric functions of the second normal stress difference $N_2(\tau, c_v)$ at different shear stresses and solid volume fractions can be written in a reduced form as found for the first normal stress difference:

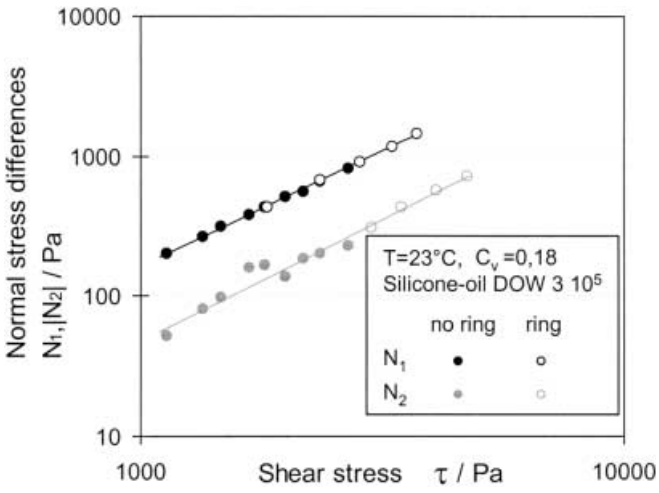

Fig. 13 Comparison of the first and second normal stress differences of glass bead suspensions based on DOW $3 \cdot 10^5$ silicone oil ($c_v = 0.18$) as a function of the imposed shear stress τ

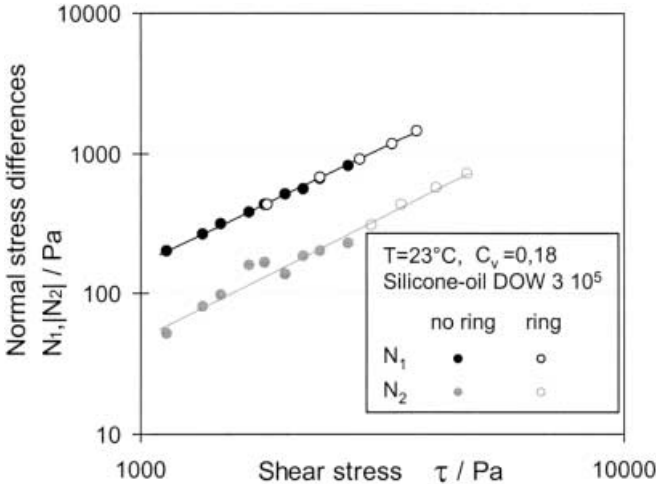

Fig. 14 Comparison of the first and second normal stress differences of glass bead suspensions based on AK 10^6 silicone oil ($c_v = 0.05$) as a function of the imposed shear stress τ

$$|N_2| = \frac{a_{N_2,m}}{B_{N_2}(c_v)} \cdot \tau^{n_2} \tag{15}$$

where $a_{N_2,m}$ is the second normal stress coefficient of the pure matrix fluid, which may not be directly measurable (as is the case for the less viscous of the two matrix fluids considered in this study).

Reduced normal stress functions $N_1^*(\tau, c_v)$ and $N_2^*(\tau, c_v)$

In Figs. 13 and 14 the first and second normal stress differences $N_1(\tau)$ and $|N_2(\tau)|$ for a suspension based on

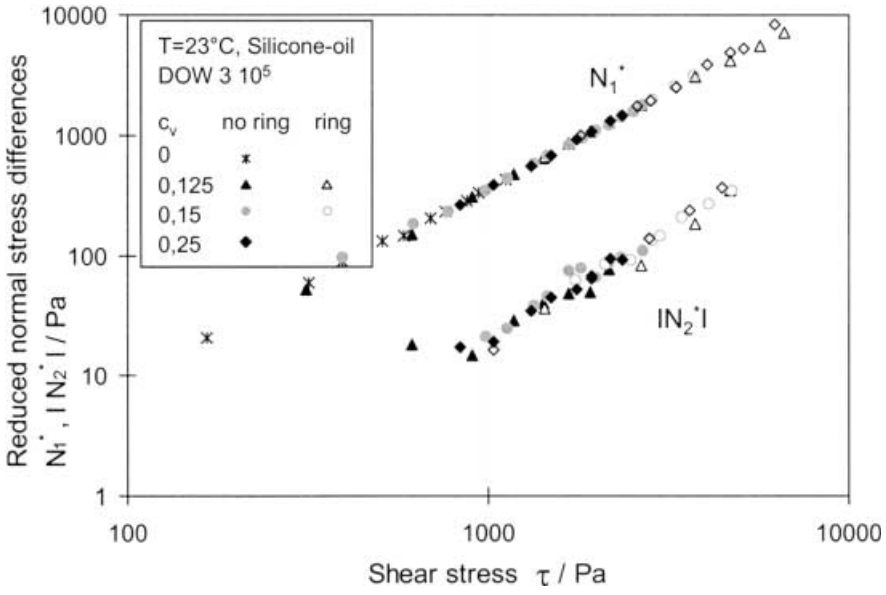

Fig. 15 Master curves of the reduced normal stress differences $N_1^*(\tau)$ and $N_2^*(\tau)$ for DOW $3 \cdot 10^5$ silicone oil and the associated suspensions

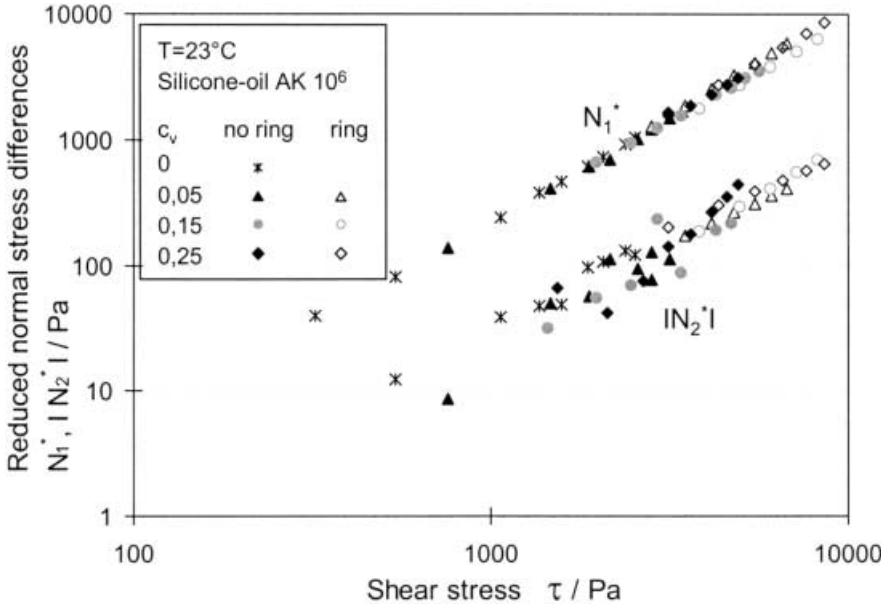

Fig. 16 Master curves of the reduced normal stress differences $N_1^*(\tau)$ and $N_2^*(\tau)$ for AK 10^6 silicone oil and the associated suspensions

Table 2 Measured power law exponents n_1 and n_2 of the normal stress functions $N_1(\tau)$ ($i = 1, 2$) for glass-bead filled suspensions using DOW $3 \cdot 10^5$ and AK 10^6 silicone oils as the viscoelastic suspending fluids

	DOW $3 \cdot 10^5$				AK 10^6			
c_v	0.0	0.125	0.15	0.25	0.0	0.125	0.15	0.25
n_1	1.56	1.61	1.64	1.70	1.66	1.70	1.58	1.70
n_2	–	1.75	1.73	1.76	1.54	1.65	1.74	1.67
$\bar{n}_1$	1.63 ± 0.06				1.66 ± 0.06			
$\bar{n}_2$	1.75 ± 0.015				1.65 ± 0.08			
$\bar{n}_{1,2}$	1.68 ± 0.008				1.66 ± 0.07			

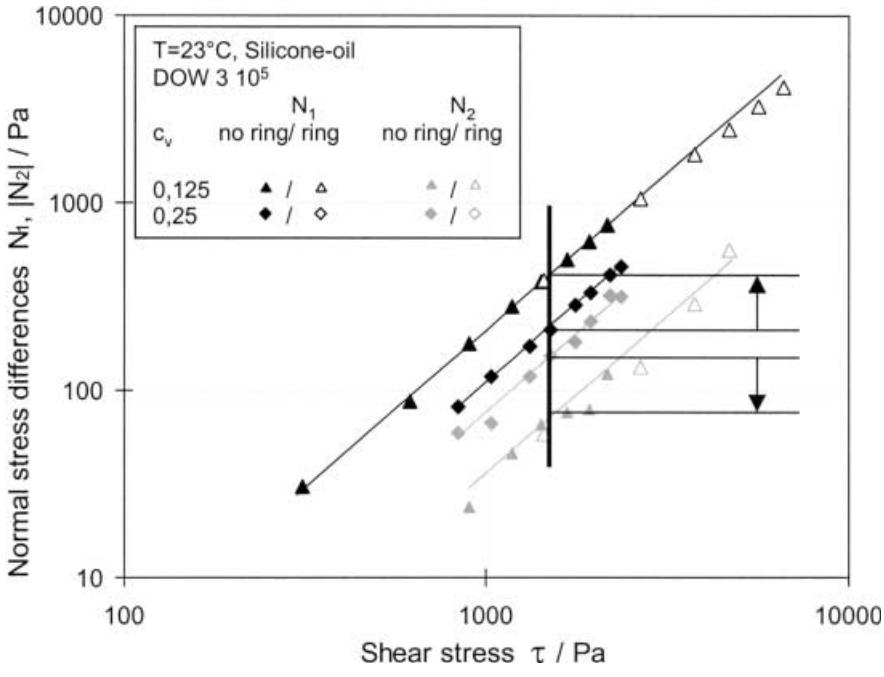

Fig. 17 Variation in the first and second normal stress differences $N_1(\tau; c_v)$ and $N_2(\tau; c_v)$ two viscoelastic suspensions formulated using DOW $3 \cdot 10^5$ silicone oil at two different volume fractions

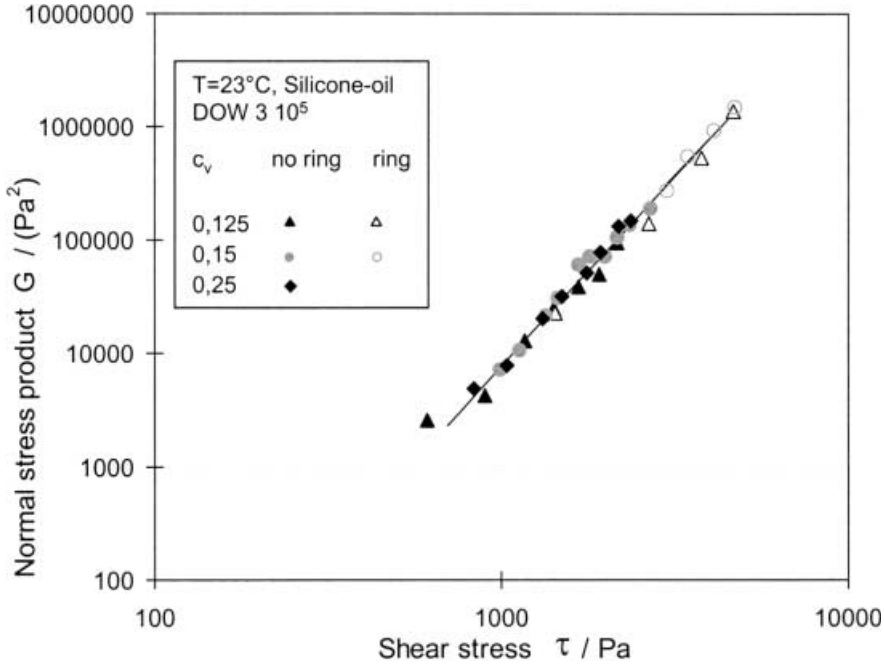

Fig. 18 The normal stress product $N_1(\tau) \cdot |N_2(\tau)| = G(\tau)$ of glass-bead filled suspensions in DOW $3 \cdot 10^5$ silicone oil

DOW $3 \cdot 10^5$ ($c_v = 0.18$) and on AK 10^6 ($c_v = 0.05$) are plotted as functions of the imposed shear stress. Once again the data are all found to be co-linear and hence we can conclude that the power law exponent in Eqs. (8), (9), (10), (12), (13) and (15) are equal to each other:

$$n_1 = n_2 = n \tag{16}$$

In these viscoelastic filled suspensions the ratio of the second normal stress difference to the first normal stress difference (denoted henceforth as Ψ^*) is thus independent of the shear stress (and shear rate) and is only a function of the volume fraction of filler:

$$\frac{|N_2(c_v, \tau)|}{N_1(c_v, \tau)} = \Psi^*(c_v) \tag{17}$$

This normal stress ratio increases with increasing solid fraction from $\Psi^*(0) \approx 0.1$ up to $\Psi^*(0.25) \approx 0.7$ for the series of suspensions formulated using the less viscous

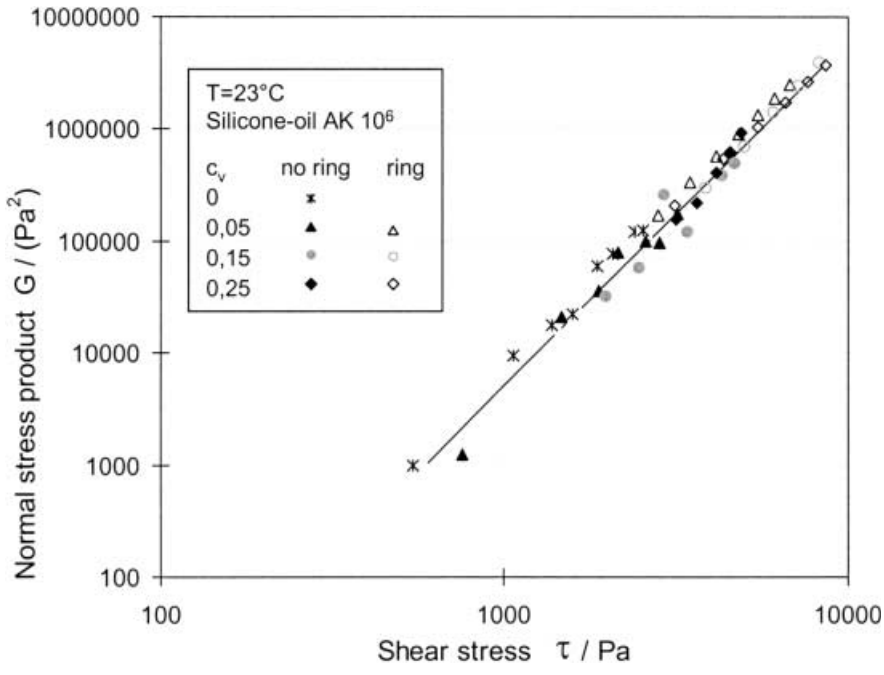

Fig. 19 The normal stress product $N_1(\tau) \cdot |N_2(\tau)| = G(\tau)$ of glass-bead filled suspensions in AK 10^6 silicone oil

Table 3 The dimensionless normal stress shift factors B_{N_1}, B_{N_2}, and their product for each series of viscoelastic suspensions

DOW $3 \cdot 10^5$				AK 10^6			
c_v	B_{N_1}	B_{N_2}	$B_{N_1} \cdot B_{N_2}$	c_v	B_{N_1}	B_{N_2}	$B_{N_1} \cdot B_{N_2}$
0.0	1	1	1	0.0	1	1	1
0.125	1.71	0.62	1.06	0.05	1.23	0.78	0.96
0.18	2.12	0.47	1.02	0.15	1.85	0.61	1.13
0.25	3.19	0.29	0.93	0.25	2.88	0.52	1.5

suspending fluid and up to 0.5 for the more viscous system.

To summarize our experimental observations so far, we have shown that, at a given value of the volume fraction, the functions $N_1(\tau)$ and $|N_2(\tau)|$ are power law functions with a common power law exponent n. The first normal stress difference N_1 is a decreasing function and $|N_2|$ is an increasing function with increasing solid fraction. Using the definitions of the first normal stress shift factor $B_{N_1}(c_v)$ from Eq. (11) and the second normal stress shift factor $B_{N_2}(c_v)$ from Eq. (14), master curves for the normal stress-shear stress functions can be found using the following relationships:

$$N_1^*(\tau) = N_1(\tau, c_v) \cdot B_{N_1}(c_v) \tag{18}$$

$$\left|N_2^*(\tau)\right| = |N_2\ (\tau, c_v)| \cdot B_{N_2}(c_v) \tag{19}$$

When the reduced normal stress differences N_1^* and $\left|N_2^*\right|$ are plotted vs the shear stress τ the data take the form shown in Figs. 15 and 16. These master curves also represent the normal stress functions of the pure matrix liquid since $B_{N_1}(c_v = 0) = B_{N_2}(c_v = 0) = 1$.

Although there is some scatter in the data (especially at low shear stresses for the AK10^6 based suspensions), the slope of the reduced functions $N_1^*(\tau)$ and $\left|N_2^*(\tau)\right|$ are found to be equal to each other. Numerical values for the power law exponents are reported in Table 2.

Normal stress inter-relationship

In Fig. 17 the first and second normal stress differences N_1 and $|N_2|$ of two suspensions with varying volume fraction of particles ($c_v = 0.125$ and $c_v = 0.25$) and a common matrix fluid (Dow $3 \cdot 10^5$) are plotted vs the shear stress τ. As noted previously $N_1(\tau)$ decreases with increasing c_v whereas $|N_2|$ increases with c_v. Close inspection of the data in Fig. 17 shows that, when plotted in double logarithmic coordinates, the relative decrease of $N_1(\tau)$ for the two volume fractions considered is nearly equal to the relative increase of $|N_2(\tau)|$ for the same solid fraction. This correlation can be formulated in the following way:

$$\frac{N_1\left(c_v^{[i]}\right)}{N_1\left(c_v^{[j]}\right)} = \left[\frac{\left|N_2\left(c_v^{[i]}\right)\right|}{\left|N_2\left(c_v^{[j]}\right)\right|}\right]^{-1} \tag{20}$$

where the superscripts i and j denote experimental data sets with two different concentrations of particles.

Comparing the shifts of N_1 and $|N_2|$ it should be taken into account that it is not the shift factors B_{N_1} and B_{N_2} themselves that are shown, but the relative change of the normal stress differences if the volume concentration is changed from $c_v = 0.125$ to $c_v = 0.25$. Two single test series are compared so that the maximum deviation of $\pm 8\%$ from equality which can be seen in the diagram is better than might be anticipated considering the complexity of the normal stress separation method.

Rearranging the experimental correlation given by Eq. (20) leads to the following very simple general interrelationship between the two normal stress differences N_1 and $|N_2|$ at two different concentrations:

$$N_1\left(c_v^{[i]}\right) \cdot \left|N_2\left(c_v^{[i]}\right)\right| = N_1\left(c_v^{[j]}\right) \cdot \left|N_2\left(c_v^{[j]}\right)\right| \tag{21}$$

To validate this relationship, the product $(N_1 \cdot |N_2|)$ was plotted vs the shear stress for both series of filled viscoelastic suspensions. A remarkably simple correlation between the normal stress differences N_1 and $|N_2|$ is thus found which can be expressed compactly in the form

$$N_1(\tau, c_v) \cdot |N_2(\tau, c_v)| = G(\tau). \tag{22}$$

i.e., the product of the first normal stress difference N_1 and the magnitude of the second normal stress difference $|N_2|$, considered at constant shear stress, is constant and independent of the solid concentration of particles within the entire shear rate range investigated. The resulting product, denoted $G(\tau)$, is a single function, rising with increasing shear stress τ for all solid fractions investigated and for both groups of suspensions (which are based on two different silicone oils and glass spheres of different mean diameter (see Figs. 18 and 19).

Using Eqs. (11), (14), and (21) it is possible to rearrange Eq. (22) in terms of the shift factors for the first and the second normal stress differences. Since these shift factors are themselves independent of the imposed stress, this relationship becomes

$$B_{N_1}(c_v) \cdot B_{N_2}(c_v) = 1 \ . \tag{23}$$

Numerical values of this product are given in Table 3. The result expressed by Eq. (23) is independent of the solid fraction c_v and holds even for the pure matrix liquid. This implies that the function $G(\tau)$ depends only on the properties of the matrix and is independent of the properties of the rigid particles used in our experiments.

As we have mentioned above it was not possible to measure directly the second normal stress difference for the less viscoelastic silicone oil (Dow $3 \cdot 10^5$). However, with the help of Eqs. (21) and (23) it is now possible, for the first time, to evaluate the magnitude of the second normal stress difference of the base (unfilled) liquid from the corresponding measurements with the (more viscoelastic) filled suspensions. Taking i as the matrix fluid and j as a data series for which both $N_1(\tau)$ and $|N_2(\tau)|$ have been measured then Eq. (21) gives

$$N_2(\tau,\, c_v = 0) \ \cong \ \left(\frac{N_1\left(\tau, c_v^{[j]}\right)}{N_1(\tau, c_v = 0)}\right) \ \left|N_2\left(\tau, c_v^{[j]}\right)\right| \ . \tag{24}$$

Using Eqs. (8), (9), and (16) the shear-stress-dependent product $G(\tau)$ can also be re-expressed in terms of the parameters characterizing the power law response of the first and second normal stress of the unfilled matrix fluid:

$$G(\tau) = a_{N_1,m} \cdot a_{N_2,m} \cdot \tau^{2n} \tag{25}$$

These relationships permit the evaluation of both the first and the second normal stress difference with respect to the shear stress and solid volume fraction, knowing simply $N_1(\tau)$ for the pure matrix fluid, the shift factor $B_{N_1}(c_v)$, and a single reference value of the function $G(\tau)$ at a reference stress τ_{ref}. For convenience, we pick a reference stress of $\tau_{ref} = 1$ kPa $= 1000$ Pa and denote this value as $G_0 \equiv G(\tau_{ref} = 1\,\text{kPa})$. It is important to recognize that only one single measurement of the second normal stress difference at any solid concentration (even at $c_v = 0$) is then sufficient to obtain the complete functional response of $N_2(\tau, c_v)$, at least in the power law regime investigated in the present study. Numerical values of the experimentally determined factors are provided in Table 4. For completeness we also summarize the complete set of equations below:

Pure matrix liquid:

$$N_1(\tau) = a_{N_1,m} \cdot \tau^n \tag{8}$$

$$N_2(\tau) = a_{N_2,m} \cdot \tau^n = \frac{(G_0/\tau_{\text{ref}}^{2n})}{a_{N_1,m}} \cdot \tau^n \tag{26}$$

Suspension:

$$N_1(\tau, c_v) = a_{N_1}(c_v) \cdot \tau^n = \frac{a_{N_1,m}}{B_{N_1}(c_v)} \cdot \tau^n \tag{12}$$

$$N_2(\tau, c_v) = a_{N_2}(c_v) \cdot \tau^n = \frac{B_{N_1}(c_v)(G_0/\tau_{\text{ref}}^{2n})}{a_{N_1,m}} \cdot \tau^n \tag{27}$$

with

$$G_0 \equiv \left(N_1\left(\tau_{ref}, c_v\right) \cdot \left|N_2\left(\tau_{ref}, c_v\right)\right|\right)_{\tau_{ref}=1kPa} \tag{22}$$

Using these simple equations and the data for a_{N_1} *and* G_0 from Table 4 plus the shift factors $B_{N_1}(c_v)$ from Table 3,

Table 4 Parameters describing the viscometric functions of filled viscoelastic suspensions. The parameters include the power-law coefficients for the matrix fluids $a_{N_i,m} \equiv a_{N_i}(c_v = 0)$ (for $i = 1, 2$), the exponent n and the normal stress factor $G_0 = G(\tau_{ref})$ at a reference value of the imposed stress (here taken to be $\tau_{ref} = 1$ kPa)

DOW $3 \cdot 10^5$				AK 10^6			
$a_{N_{1,m}}$ $Pa^{(1-n)}$	$a_{N_{2,m}}$ $Pa^{(1-n)}$	n –	G_0 kPa^2	$a_{N_{1,m}}$ $Pa^{(1-n)}$	$a_{N_{2,m}}$ $Pa^{(1-n)}$	n –	G_0 kPa^2
$3.5 \cdot 10^{-3}$	$2 \cdot 10^{-4}$	1.68	7.93	$2.3 \cdot 10^{-3}$	$2.2 \cdot 10^{-4}$	1.66	4.59

the complete set of normal stress functions can be calculated. The calculations are presented in Figs. 20 and 21. Considering the significant experimental problems associated with normal stress measurements, very good agreement is obtained between the calculations (lines) and the measurements (symbols).

In Table 5 the resulting normal stress ratios $\Psi^*(c_v) = |N_2|/N_1$ for DOW $3 \cdot 10^5$ and AK 10^6 and their corresponding suspensions are given. This ratio increases monotonically with increasing solid fraction from values of O (10^{-1}) which are characteristic unfilled viscoelastic melts to values greater than 0.5 at high volume fraction.

It is possible to predict the normal stress behaviour of viscoelastic suspensions with only three parameters: $a_{N_1}(c_v)$ (or equivalently $a_{N_{1,m}}$ and the shift factor $B_{N_1}(c_v)$, the constant slope n, and the reference value of the normal stress product G_0. The values of the slope n for the normal stress shear stress power law functions result in $n = 1.68$ for DOW $3 \cdot 10^5$ and $n = 1.66$ for AK 10^6. These values are very close to each other and within the range of experimental error. Tanaka and White (1980) give a value of $n = 1.67$ for Polystyrene, Ohl and Gleissle (1993) measured $n = 1.65$ for silicone oils and $n = 1.63$ for polyisobutene. For all of these materials n is in the small range of $1.63 \le n \le 1.68$ and hence seems to be independent of the matrix material. Taking this value as a universal exponent the present experiments suggest that there are only two parameters remaining (i.e., $a_{N_1}(c_v)$ and G_0) which have to be determined. The normal stress product G_0 characterizes the matrix liquid, and the factor $a_{N_1}(c_v)$ (or equivalently the normal stress shift factor $B_{N_1}(c_v)$) depends only on the properties of the filler material. It should be noted that smaller values of n have been reported for other filled materials (Liang and Li 1999; Markovic et al. 2000); however, these values have typically been inferred from indirect measurements in non-viscometric flows, rather than measured directly in torsional rheometers.

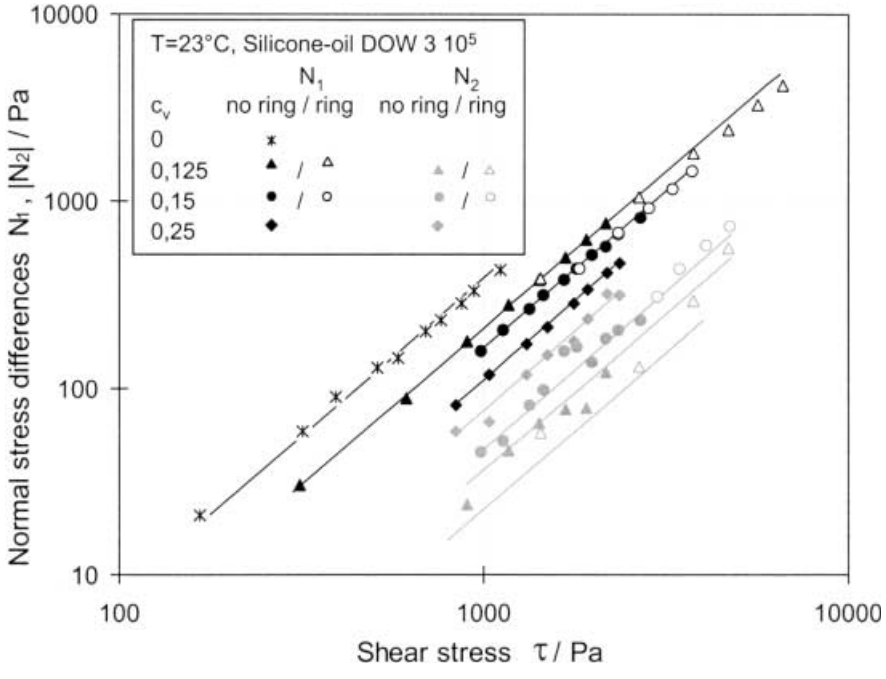

Fig. 20 Comparison of the experimentally measured (*symbols*) and predicted (*lines*) values of the first and second normal stress differences $N_1(\tau, c_v)$ and $N_2(\tau, c_v)$ for DOW $3 \cdot 10^5$ silicone oil suspensions as a function of the shear stress and volume fraction

Table 5 The normal stress difference ratio $\Psi^*(c_v) = |N_2|/N_1$ as a function of the volume fraction of filler for suspensions based on two silicone oils (DOW $3 \cdot 10^5$, and AK 10^6) of differing viscosities

DOW $3 \cdot 10^6$		AK 10^6	
c_v	$\|N_2\|$ N_1	c_v	$\|N_2\|$ N_1
0.0	0.06	0.0	0.1
0.125	0.17	0.05	0.15
0.18	0.29	0.15	0.29
0.25	0.69	0.25	0.52

Conclusions

In this work we have systematically measured the variation in the normal stress differences for highly filled suspensions formulated with viscoelastic matrix liquids. We have demonstrated in these experiments that simple inter-relations between the viscometric functions appear to exist for filled viscoelastic suspensions. Measurements of the first normal stress difference $N_1(\tau, c_v)$ are in good agreement with earlier investigations. To our knowledge, the measurements of the changes in the second normal stress difference $N_2(\tau, c_v)$ with respect to imposed shear stress and increasing solid volume fraction represent the first such data. The measurements indicate that, for the viscoelastic silicone oil matrix fluids used in the present studies, N_2 is negative for all samples tested whereas N_1 is positive. By contrast, recent measurements at high Peclet numbers in viscous Newtonian solvents have shown that both of the normal stress differences were negative with $|N_2| > |N_1|$ (Zarraga et al. 2000). Measurements by Aral and Kalyon (1997) also indicated that, after a long transient, the steady state first normal stress difference was negative for a silicone oil filled with glass beads. The matrix fluid used by the latter authors was significantly less viscous than the matrix fluids utilized in the present study and presumably is thus also less viscoelastic. In addition Aral and Kalyon report that the normal stresses could only be measured reliably for volume fractions in excess of 30%.

In agreement with previous publications using viscoelastic suspending fluids at moderate volume fractions ($c_v \leq 0.25$) we find that the first normal stress difference is positive but decreases with increasing solid content (when compared at constant shear stresses). The picture that is thus emerging suggests that the first normal stress difference is comprised of two (additive) terms; one positive term arising from the matrix fluid (with magnitude depending on the molecular weight of the polymeric material forming the solvent) and a second, negative, term with magnitude varying with the volume fraction of solid suspended. The magnitude of the normal stresses in a suspension at high Peclet number are expected to scale with the viscosity of the suspension and the imposed shear rate (Brady and Vicic 1995), and can thus be represented as a function of the imposed shear stress. Furthermore, over the range of shear stresses applied in the present investigation, the normal stress/shear stress functions can be approximated by simple power law equations with a common exponent that is independent of the solid fraction and hence characterizes both the matrix liquid

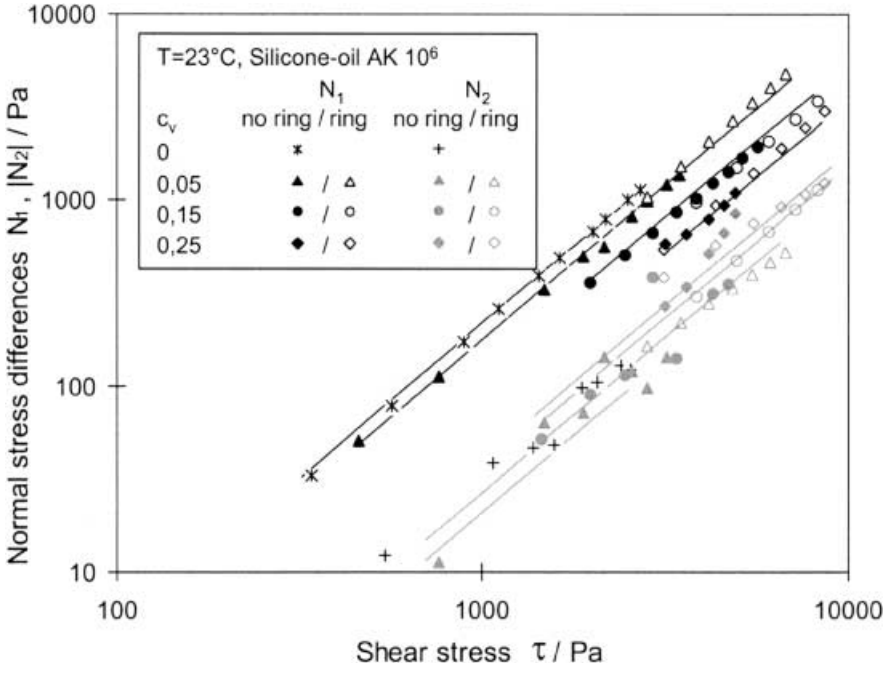

Fig. 21 Comparison of the experimentally measured (*symbols*) and predicted (*lines*) values of the first and second normal stress differences $N_1(\tau, c_v)$ and $N_2(\tau, c_v)$ for AK 10^6 silicone oil suspensions as a function of the shear stress and volume fraction

and the filled suspension. This suggests the following simple functional form for the first normal stress difference:

$$N_1(\tau, c_v) \equiv N_{1,matrix} + N_{1,susp} \approx a_{1m}\tau^n[1 - g(c_v)] \quad (28)$$

where the shift factor we have determined experimentally is thus $B_{N_1} \equiv [1 - g(c_v)]^{-1}$. The sign of the first normal stress difference thus depends on the magnitude of the normal stresses in the unfilled polymeric solvent and on the volume fraction of filler.

The data presented in this study show that the magnitude of the second normal stress difference monotonically increases with rising solid fraction. Additionally it was found that, when compared at constant shear stress, the relative decrease of N_1 with c_v is equal to the relative increase of $|N_2|$. To be consistent with these observations, we should thus expect for the range of volume fractions and stresses considered that:

$$N_2(\tau, c_v) = N_{2,m} + N_{2,susp} \approx -\frac{a_{2m}\tau^n}{[1 - g(c_v)]} \quad (29)$$

With these functional forms, the product of the normal stress differences $N_1(\tau, c_v) \cdot |N_2(\tau, c_v)| = G(\tau)$ is only a function of the external shear stress imposed on the system; i.e., it is independent of the volume fraction of particles added to the fluid, and is equal to the product of the normal stress differences at $c_v = 0$. These predicted forms for the normal stress differences are consistent with experimental observations made to date in viscoelastic suspensions but have yet to be verified by microstructural theory.

The viscometric functions for the normal stress differences of filled viscoelastic suspensions is thus predictable with only three parameters:

1. $a_{N_1}(c_v)$; the front factor of the power law equation describing the variation in $N_1(\tau, c_v)$ at the required volume fraction
2. The power law exponent n itself
3. The normal stress difference product $G_0 = N_1(\tau, c_v) \cdot |N_2(\tau, c_v)|$ at a reference stress; e.g. at $\tau_{ref} = 1$ kPa

An appreciable advantage of these simple correlations from the perspective of polymer processing operations is the possibility to calculate approximately $N_2(\tau, c_v)$ by measuring only $N_1(\tau, c_v)$ and knowing the normal stress product. If the latter quantity is unknown, the data in Table 5 can be utilized to provide an estimate for the ratio $\Psi^*(c_v)$. It should be emphasized that these simple correlations hold for viscoelastic filled materials in the range of very high Peclet numbers in which the microstructural deformation is governed only by hydrodynamic forces. These simple power-law relationships and shift factors may be used to interpolate and predict the expected form of the material functions for other values of the volume fraction $0 \le c_v \le 0.5$. They may also be useful in guiding constitutive modeling of the rheology of filled suspensions.

Acknowledgements This work was completed during the visit of S. Gleissle to Harvard and M.I.T. The authors also extend their thanks to Prof. Robert C. Armstrong from the Department of Chemical Engineering of Massachusetts Institute of Technology Cambridge, MA for the use of the rheological equipment in his laboratory.

References

Aral BK, Kalyon DM (1997) Viscoelastic material functions of noncolloidal suspensions with spherical particles. J Rheol 41(3):599–620

Bird RB, Armstrong RC, Hassager O (1987) Dynamics of polymeric liquids. Vol 1: Fluid mechanics. Wiley Interscience, New York

Brady JF, Vicic M (1995) Normal stresses in colloidal dispersions. J Rheol 39(3):545–66

Foss DR, Brady JF (2000) Brownian dynamics simulation of hard-sphere colloidal dispersions. J Rheol 44(3):629–651

Gleissle S, Gleissle W, McKinley GH, Buggisch H (1998) The normal stress behaviour of suspensions with viscoelastic matrix fluids. Proceedings of 5th European Rheology Congress, Portorosc, Slovenia, pp 554–555

Gleissle S, Gleissle W, McKinley GH, Buggisch H (2000) The normal stress behaviour of suspensions with viscoelastic matrix fluids. Proceedings of 13th International Congress on Rheology, Cambridge, UK, vol II, pp 262–264

Gleissle W (1974) Schub- und Normalspannungsmessungen an Silikonölen bei hohen Schergeschwindigkeiten mit einem neuen Kegel-Platte-Rheometer. Colloid Polym Sci 252:848–885

Gleissle W (1976) Druckverteilung im Spalt eines Kegel-Platte-Rheometers bei der Scherung viskoelastischer Flüssigkeiten mit hohen Schergeschwindigkeiten. Rheol Acta 15:305–316

Gleissle W (1978) Ein Kegel-Platte-Rheometer für zähe viskoelastische Flüssigkeiten bei hohen Schergeschwindigkeiten, Untersuchungen des Fliessverhaltens von hochmolekularem Silikonöl und Polyisobutylen. Diss. Universitaet Karlsruhe (TH), Karlsruhe

Gleissle W (1996) Transient and steady state shear and normal stresses in concentrated suspensions. Proceedings of the 12th International Congress on Rheology, Quebec City, Canada, pp 538–539

Gleissle W, Baloch MK (1984) Reduced flow functions of suspensions based on Newtonian- and non-Newtonian liquids. Proceedings of the IXth International Congress on Rheology, Acapulco, Mexico, vol 2, pp 549–556

Hornsby PR (1999) Rheology, compounding and processing of filled thermoplastics. Adv Polym Sci 139:155–217

Hutton SF (1969) Fracture and secondary flow of elastic liquids. Rheol Acta 8:54–59

Keentok M, Xue SC (1999) Edge fracture in cone-plate and parallel plate flows. Rheol Acta 38(4):321–348

Kotaka T, Kurata M, Tamura M (1959) Normal stress effect in polymer solutions. J Appl Phys 30:1705–1712

Lee CS, Tripp BC, Magda JJ (1992) Does N1 or N2 control the onset of edge fracture. Rheol Acta 31:306–398

Liang JZ, Li RKY (1999) Rheological properties of glass bead-filled low-density polyethylene composite melts in capillary extrusion. J Appl Polym Sci 73(8):1451–1456

Markovic MG, Choudhury NR, Dimopoulos M, Matisons JG, Dutta NK, Bhattacharya AK. (2000) Rheological behavior of highly filled ethylene propylene diene rubber compounds. Polym Eng Sci 40(5):1065–1073

Meissner J, Garbella RW, Hostettler J (1989) Measuring normal stress differences in polymer melt shear flow. J Rheol 33:843–864

Ohl N (1991) Die Beschreibung des Fliessverhaltens von Suspensionen viskoelastischer Flüssigkeiten bis zu hohen Volumenkonzentrationen. Diss. Universität Karlsruhe (TH), Karlsruhe

Ohl N, Gleissle W (1992) The second normal stress difference for pure and highly filled viscoelastic fluids. Rheol Acta 31:294–306

Ohl N, Gleissle W (1993) The characterization of steady-state shear and normal stress functions of highly concentrated suspensions formulated with viscoelastic liquids. J Rheol 37(2):381–406

Petersen FJ (1974) Zur Bestimmung der Normalspannungsfunktionen von Hochpolymeren mittels der Platte-Abstands-Anordnung. Diss. RWTH-Aachen, Aachen

Phan-Thien N, Fan XJ, Khoo BC (1999) A new constitutive model for monodispersed suspensions of spheres at high concentrations. Rheol Acta 38(4):297–304

Powell RL (1998) In: Collyer AA, Clegg PW (eds) Rheological measurements. Chapman & Hall, London

Schaink HM, Slot JM, Jongschaap RJJ, Mellema J (2000) The rheology of systems containing rigid spheres suspended in both viscous and viscoelastic media, studied by Stokesian dynamics simulations. J Rheol 44(3):473–498

Tanaka H, White JL (1980) Experimental investigations of shear and elongational flow properties of polystyrene melts reinforced with calcium carbonate, titanium dioxide, and carbon black. Polym Eng Sci 20:949–956

Tanner RI, Keentok M (1983) Shear fracture in cone-plate rheometry. J Rheol 27:47–57

Zarraga IE, Hill DA, Leighton DT (2000) The characterization of the total stress of concentrated suspensions of noncolloidal spheres in Newtonian fluids. J Rheol 44(2):185–220